

Structure of Low-Lying Baryon Resonances

Derek Leinweber

In collaboration with: Curtis Abell, Liam Hockley, Waseem Kamleh,
Yan Li, Zhan-Wei Liu, Finn Stokes, Tony Thomas, Jia-Jun Wu



THE UNIVERSITY
of ADELAIDE

Outline

- Hamiltonian Effective Field Theory (HEFT)
 - Nonperturbative extension of chiral effective field theory aimed at resonance physics.
 - Incorporates the Lüscher formalism.
 - Connects scattering observables to the finite-volume spectrum of lattice QCD.
- Δ Resonance: introduce HEFT and illustrate the constraints provided by Lüscher.
 - Discuss the role of lattice QCD results in constraining the description of multi-channel scattering processes.
- Odd-parity $N^*(1535)$ and $N^*(1650)$ Resonances:
 - Knowledge of eigenstate composition can be used to understand lattice QCD results.
- Roper $N(1440)$ Resonance:
 - Lattice QCD results constrain the HEFT description of experimental data.
 - Provides deep insight into the nature of the Roper resonance.
- Conclusions

Hamiltonian Effective Field Theory (HEFT)

J. M. M. Hall, *et al.* [CSSM], Phys. Rev. D **87** (2013) 094510 [[arXiv:1303.4157 \[hep-lat\]](https://arxiv.org/abs/1303.4157)]
C. D. Abell, D. B. L., A. W. Thomas and J. J. Wu, Phys. Rev. D **106** (2022) 034506 [[arXiv:2110.14113 \[hep-lat\]](https://arxiv.org/abs/2110.14113)]

- An extension of chiral effective field theory incorporating the Lüscher formalism
 - Linking the energy levels observed in finite volume to scattering observables.

Hamiltonian Effective Field Theory (HEFT)

J. M. M. Hall, *et al.* [CSSM], Phys. Rev. D **87** (2013) 094510 [[arXiv:1303.4157 \[hep-lat\]](https://arxiv.org/abs/1303.4157)]
C. D. Abell, D. B. L., A. W. Thomas and J. J. Wu, Phys. Rev. D **106** (2022) 034506 [[arXiv:2110.14113 \[hep-lat\]](https://arxiv.org/abs/2110.14113)]

- An extension of chiral effective field theory incorporating the Lüscher formalism
 - Linking the energy levels observed in finite volume to scattering observables.
- In the light quark-mass regime, in the perturbative limit,
 - HEFT reproduces the finite-volume expansion of chiral perturbation theory.

Hamiltonian Effective Field Theory (HEFT)

J. M. M. Hall, *et al.* [CSSM], Phys. Rev. D **87** (2013) 094510 [[arXiv:1303.4157 \[hep-lat\]](https://arxiv.org/abs/1303.4157)]
C. D. Abell, D. B. L., A. W. Thomas and J. J. Wu, Phys. Rev. D **106** (2022) 034506 [[arXiv:2110.14113 \[hep-lat\]](https://arxiv.org/abs/2110.14113)]

- An extension of chiral effective field theory incorporating the Lüscher formalism
 - Linking the energy levels observed in finite volume to scattering observables.
- In the light quark-mass regime, in the perturbative limit,
 - HEFT reproduces the finite-volume expansion of chiral perturbation theory.
- Fitting resonance phase-shift data and inelasticities,
 - Predictions of the finite-volume spectrum are made.

Hamiltonian Effective Field Theory (HEFT)

J. M. M. Hall, *et al.* [CSSM], Phys. Rev. D **87** (2013) 094510 [[arXiv:1303.4157 \[hep-lat\]](https://arxiv.org/abs/1303.4157)]
C. D. Abell, D. B. L., A. W. Thomas and J. J. Wu, Phys. Rev. D **106** (2022) 034506 [[arXiv:2110.14113 \[hep-lat\]](https://arxiv.org/abs/2110.14113)]

- An extension of chiral effective field theory incorporating the Lüscher formalism
 - Linking the energy levels observed in finite volume to scattering observables.
- In the light quark-mass regime, in the perturbative limit,
 - HEFT reproduces the finite-volume expansion of chiral perturbation theory.
- Fitting resonance phase-shift data and inelasticities,
 - Predictions of the finite-volume spectrum are made.
- The eigenvectors of the Hamiltonian provide insight into the composition of the energy eigenstates.
 - Insight is similar to that provided by correlation-matrix eigenvectors in Lattice QCD.

Infinite Volume Model

- The rest-frame Hamiltonian has the form $H = H_0 + H_I$, with

$$H_0 = \sum_{B_0} |B_0\rangle m_{B_0} \langle B_0| + \sum_{\alpha} \int d^3k |\alpha(\mathbf{k})\rangle \omega_{\alpha}(\mathbf{k}) \langle \alpha(\mathbf{k})|,$$

Infinite Volume Model

- The rest-frame Hamiltonian has the form $H = H_0 + H_I$, with

$$H_0 = \sum_{B_0} |B_0\rangle m_{B_0} \langle B_0| + \sum_{\alpha} \int d^3k |\alpha(\mathbf{k})\rangle \omega_{\alpha}(\mathbf{k}) \langle \alpha(\mathbf{k})|,$$

- $|B_0\rangle$ denotes a quark-model-like basis state.

Infinite Volume Model

- The rest-frame Hamiltonian has the form $H = H_0 + H_I$, with

$$H_0 = \sum_{B_0} |B_0\rangle m_{B_0} \langle B_0| + \sum_{\alpha} \int d^3k |\alpha(\mathbf{k})\rangle \omega_{\alpha}(\mathbf{k}) \langle \alpha(\mathbf{k})|,$$

- $|B_0\rangle$ denotes a quark-model-like basis state.
- $|\alpha(\mathbf{k})\rangle$ designates a two-particle non-interacting basis-state channel with energy

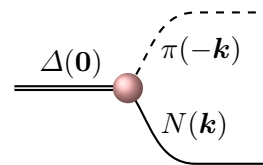
$$\omega_{\alpha}(\mathbf{k}) = \omega_{\alpha_M}(\mathbf{k}) + \omega_{\alpha_B}(\mathbf{k}) = \sqrt{\mathbf{k}^2 + m_{\alpha_M}^2} + \sqrt{\mathbf{k}^2 + m_{\alpha_B}^2},$$

for $M = \text{Meson}$, $B = \text{Baryon}$.

Infinite Volume Model

- The interaction Hamiltonian includes two parts, $H_I = g + v$.
- $1 \rightarrow 2$ particle vertex

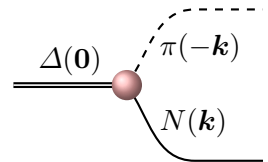
$$g = \sum_{\alpha, B_0} \int d^3k \left\{ |\alpha(\mathbf{k})\rangle G_{\alpha, B_0}^\dagger(k) \langle B_0| + h.c. \right\},$$



Infinite Volume Model

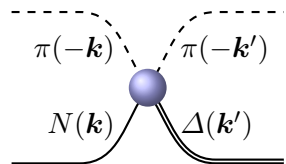
- The interaction Hamiltonian includes two parts, $H_I = g + v$.
- $1 \rightarrow 2$ particle vertex

$$g = \sum_{\alpha, B_0} \int d^3k \left\{ |\alpha(\mathbf{k})\rangle G_{\alpha, B_0}^\dagger(k) \langle B_0| + h.c. \right\},$$



- $2 \rightarrow 2$ particle vertex

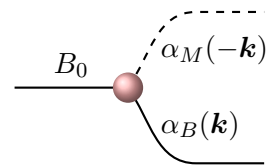
$$v = \sum_{\alpha, \beta} \int d^3k d^3k' |\alpha(\mathbf{k})\rangle V_{\alpha, \beta}^S(k, k') \langle \beta(\mathbf{k}')|.$$



S-wave vertex interactions

- *S*-wave vertex interactions between the one baryon and two-particle meson-baryon channels for e.g. $N^*(1535)$ or $\Lambda^*(1405)$ cases take the form

$$G_{\alpha, B_0}(k) = g_{B_0 \alpha} \frac{\sqrt{3}}{2 \pi f_\pi} \sqrt{\omega_{\alpha_M}(k)} u(k, \Lambda),$$



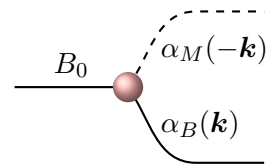
with regulator

$$u(k, \Lambda) = \left(1 + \frac{k^2}{\Lambda^2} \right)^{-2}, \quad \text{and fixed } \Lambda \sim 0.8 \rightarrow 1.0 \text{ GeV.}$$

P-wave and higher vertex interactions

- P-wave vertex interactions between the one baryon and two-particle meson-baryon channels for e.g. for the $\Delta(1232)$ or $N^*(1440)$ case cases take the form

$$G_{\alpha, B_0}(k) = g_{B_0 \alpha} \frac{1}{4\pi^2} \left(\frac{k}{f_\pi}\right)^{l_\alpha} \frac{u(k, \Lambda)}{\sqrt{\omega_{\alpha_M}(k)}},$$



where l_α is the orbital angular momentum in channel α .

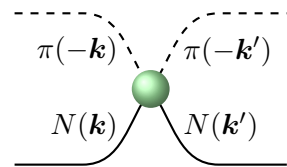
Two-to-two particle interactions

- For the direct two-to-two particle interaction, we introduce separable potentials.

Two-to-two particle interactions

- For the direct two-to-two particle interaction, we introduce separable potentials.
- For the S_{11} πN channel

$$V_{\pi N, \pi N}^S(k, k') = v_{\pi N, \pi N} \frac{3}{4\pi^2 f_\pi^2} \tilde{u}_{\pi N}(k, \Lambda) \tilde{u}_{\pi N}(k', \Lambda)$$



where the scattering potential gains a low energy enhancement via

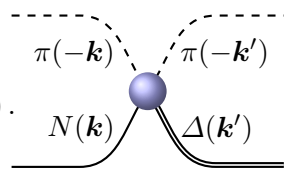
$$\tilde{u}_{\pi N}(k, \Lambda) = u(k, \Lambda) \frac{m_\pi^{\text{phys}} + \omega_\pi(k)}{\omega_\pi(k)}$$

and $u(k, \Lambda)$ takes the dipole form.

Two-to-two particle interactions

- For P -wave scattering in the $\Delta(1232)$ or $N^*(1440)$ channels

$$V_{\alpha,\beta}^S(k, k') = v_{\alpha,\beta} \frac{1}{4\pi^2 f_\pi^2} \frac{k}{\omega_{\alpha_M}(k)} \frac{k'}{\omega_{\beta_M}(k')} u(k, \Lambda) u(k', \Lambda).$$



Infinite-Volume scattering amplitude

- The T -matrices for two particle scattering are obtained by solving the coupled-channel integral equations

$$T_{\alpha,\beta}(k, k'; E) = \tilde{V}_{\alpha,\beta}(k, k'; E) + \sum_{\gamma} \int q^2 dq \frac{\tilde{V}_{\alpha,\gamma}(k, q; E) T_{\gamma,\beta}(q, k'; E)}{E - \omega_{\gamma}(q) + i\epsilon}.$$

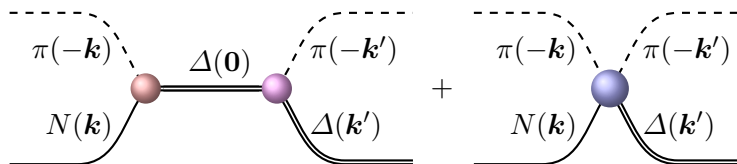
Infinite-Volume scattering amplitude

- The T -matrices for two particle scattering are obtained by solving the coupled-channel integral equations

$$T_{\alpha,\beta}(k, k'; E) = \tilde{V}_{\alpha,\beta}(k, k'; E) + \sum_{\gamma} \int q^2 dq \frac{\tilde{V}_{\alpha,\gamma}(k, q; E) T_{\gamma,\beta}(q, k'; E)}{E - \omega_{\gamma}(q) + i\epsilon}.$$

- The coupled-channel potential is readily calculated from the interaction Hamiltonian

$$\tilde{V}_{\alpha,\beta}(k, k') = \sum_{B_0} \frac{G_{\alpha,B_0}^{\dagger}(k) G_{\beta,B_0}(k')}{E - m_{B_0}} + V_{\alpha,\beta}^S(k, k'),$$



Infinite-Volume scattering matrix

- The S -matrix is related to the T -matrix by

$$S_{\alpha,\beta}(E) = 1 - 2i \sqrt{\rho_\alpha(E) \rho_\beta(E)} T_{\alpha,\beta}(k_{\alpha \text{ cm}}, k_{\beta \text{ cm}}; E),$$

with

$$\rho_\alpha(E) = \pi \frac{\omega_{\alpha_M}(k_{\alpha \text{ cm}}) \omega_{\alpha_B}(k_{\alpha \text{ cm}})}{E} k_{\alpha \text{ cm}},$$

and $k_{\alpha \text{ cm}}$ satisfies the on-shell condition

$$\omega_{\alpha_M}(k_{\alpha \text{ cm}}) + \omega_{\alpha_B}(k_{\alpha \text{ cm}}) = E.$$

Infinite-Volume scattering matrix

- The S-matrix is related to the T-matrix by

$$S_{\alpha,\beta}(E) = 1 - 2i \sqrt{\rho_\alpha(E) \rho_\beta(E)} \, T_{\alpha,\beta}(k_{\alpha \text{ cm}}, k_{\beta \text{ cm}}; E),$$

with

$$\rho_\alpha(E) = \pi \frac{\omega_{\alpha_M}(k_{\alpha \text{ cm}}) \omega_{\alpha_B}(k_{\alpha \text{ cm}})}{E} k_{\alpha \text{ cm}},$$

and $k_{\alpha \text{ cm}}$ satisfies the on-shell condition

$$\omega_{\alpha_M}(k_{\alpha \text{ cm}}) + \omega_{\alpha_B}(k_{\alpha \text{ cm}}) = E.$$

- The cross section $\sigma_{\alpha,\beta}$ for the process $\alpha \rightarrow \beta$ is

$$\sigma_{\alpha,\beta} = \frac{4\pi^3 k_{\alpha \text{ cm}} \omega_{\alpha_M}(k_{\alpha \text{ cm}}) \omega_{\alpha_B}(k_{\alpha \text{ cm}}) \omega_{\beta_M}(k_{\alpha \text{ cm}}) \omega_{\beta_B}(k_{\alpha \text{ cm}})}{E^2 k_{\beta \text{ cm}}} |T_{\alpha,\beta}(k_{\alpha \text{ cm}}, k_{\beta \text{ cm}}; E)|^2.$$

πN phase shift and inelasticity

- The S-matrix is related to the T-matrix by

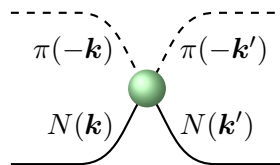
$$\begin{aligned} S_{\pi N, \pi N}(E) &= 1 - 2i\pi \frac{\omega_\pi(k_{\text{cm}}) \omega_N(k_{\text{cm}})}{E} k_{\text{cm}} T_{\pi N, \pi N}(k_{\text{cm}}, k_{\text{cm}}; E), \\ &= \eta(E) e^{2i\delta(E)}. \end{aligned}$$

πN phase shift and inelasticity

- The S-matrix is related to the T-matrix by

$$\begin{aligned} S_{\pi N, \pi N}(E) &= 1 - 2i\pi \frac{\omega_\pi(k_{\text{cm}}) \omega_N(k_{\text{cm}})}{E} k_{\text{cm}} T_{\pi N, \pi N}(k_{\text{cm}}, k_{\text{cm}}; E), \\ &= \eta(E) e^{2i\delta(E)}. \end{aligned}$$

- In solving for the energy eigenstates...

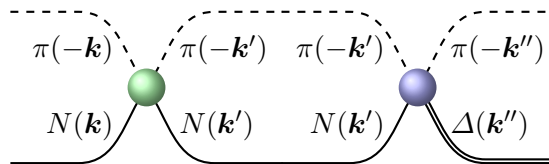


πN phase shift and inelasticity

- The S-matrix is related to the T-matrix by

$$\begin{aligned}
 S_{\pi N, \pi N}(E) &= 1 - 2i\pi \frac{\omega_\pi(k_{\text{cm}}) \omega_N(k_{\text{cm}})}{E} k_{\text{cm}} T_{\pi N, \pi N}(k_{\text{cm}}, k_{\text{cm}}; E), \\
 &= \eta(E) e^{2i\delta(E)}.
 \end{aligned}$$

- In solving for the energy eigenstates...

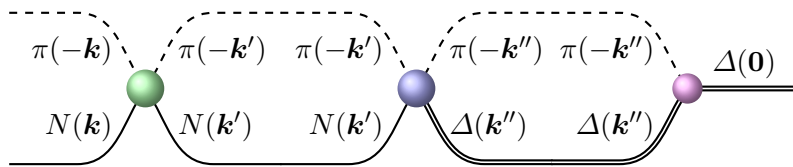


πN phase shift and inelasticity

- The S-matrix is related to the T-matrix by

$$\begin{aligned}
 S_{\pi N, \pi N}(E) &= 1 - 2i\pi \frac{\omega_\pi(k_{\text{cm}}) \omega_N(k_{\text{cm}})}{E} k_{\text{cm}} T_{\pi N, \pi N}(k_{\text{cm}}, k_{\text{cm}}; E), \\
 &= \eta(E) e^{2i\delta(E)}.
 \end{aligned}$$

- In solving for the energy eigenstates...

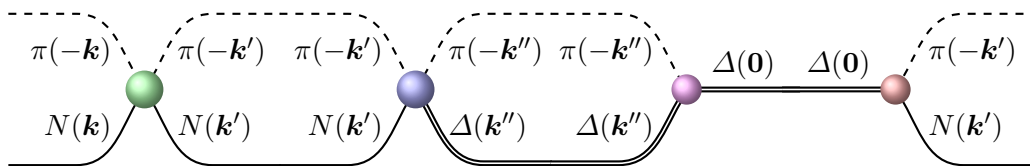


πN phase shift and inelasticity

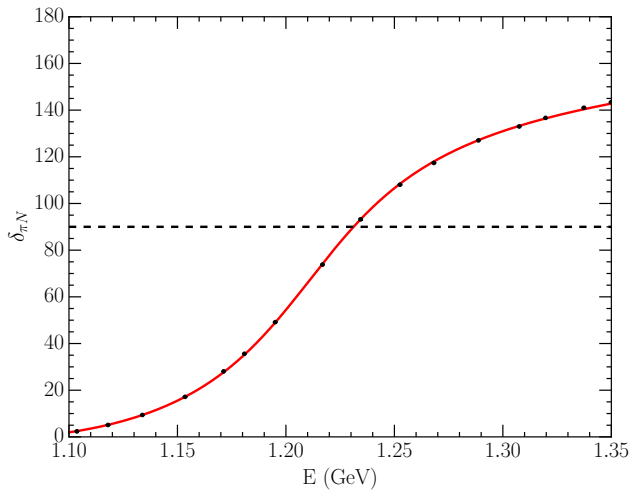
- The S-matrix is related to the T-matrix by

$$\begin{aligned} S_{\pi N, \pi N}(E) &= 1 - 2i\pi \frac{\omega_\pi(k_{\text{cm}}) \omega_N(k_{\text{cm}})}{E} k_{\text{cm}} T_{\pi N, \pi N}(k_{\text{cm}}, k_{\text{cm}}; E), \\ &= \eta(E) e^{2i\delta(E)}. \end{aligned}$$

- In solving for the energy eigenstates...



P-wave πN phase shifts in the Δ channel - 1 πN channel



Finite Volume Analysis

- In a finite periodic volume, momentum is quantised to $n (2\pi/L)$.

Finite Volume Analysis

- In a finite periodic volume, momentum is quantised to $n (2\pi/L)$.
- In a cubic volume of extent L on each side, define the momentum magnitudes

$$k_n = \sqrt{n_x^2 + n_y^2 + n_z^2} \frac{2\pi}{L},$$

with $n_i = 0, 1, 2, \dots$ and integer $n = n_x^2 + n_y^2 + n_z^2$.

Finite Volume Analysis

- In a finite periodic volume, momentum is quantised to $n (2\pi/L)$.
- In a cubic volume of extent L on each side, define the momentum magnitudes

$$k_n = \sqrt{n_x^2 + n_y^2 + n_z^2} \frac{2\pi}{L},$$

with $n_i = 0, 1, 2, \dots$ and integer $n = n_x^2 + n_y^2 + n_z^2$.

- The non-interacting Hamiltonian takes the form

$$H_0 = \begin{pmatrix} m_{B_0} & 0 & 0 & \cdots \\ \omega_{\pi N}(k_0) & \ddots & 0 & \cdots \\ 0 & \ddots & \ddots & \cdots \\ & & \omega_{\pi \Delta}(k_0) & \cdots \\ & & & \omega_{\pi N}(k_1) \\ 0 & 0 & \ddots & \cdots \\ & & & \omega_{\pi \Delta}(k_1) \\ \vdots & \vdots & \vdots & \ddots \end{pmatrix}.$$

1 → 2 particle interaction terms

- 1 → 2 particle interaction terms sit in the first row and column.

$$H_I = \begin{pmatrix} 0 & g_{\pi N}(k_0) & \cdots & g_{\pi\Delta}(k_0) & g_{\pi N}(k_1) & \cdots & g_{\pi\Delta}(k_1) \cdots \\ g_{\pi N}(k_0) & 0 & \cdots & & & & \\ \vdots & \vdots & 0 & & & & \\ g_{\pi\Delta}(k_0) & & & \ddots & & & \\ g_{\pi N}(k_1) & & & & & & \\ \vdots & & & & & & \\ g_{\pi\Delta}(k_1) & & & & & & \\ \vdots & & & & & & \end{pmatrix}.$$

1 → 2 particle interaction terms

- 1 → 2 particle interaction terms sit in the first row and column.

$$H_I = \begin{pmatrix} 0 & g_{\pi N}(k_0) & \cdots & g_{\pi\Delta}(k_0) & g_{\pi N}(k_1) & \cdots & g_{\pi\Delta}(k_1) \cdots \\ g_{\pi N}(k_0) & 0 & \cdots & & & & \\ \vdots & \vdots & 0 & & & & \\ g_{\pi\Delta}(k_0) & & & \ddots & & & \\ g_{\pi N}(k_1) & & & & & & \\ \vdots & & & & & & \\ g_{\pi\Delta}(k_1) & & & & & & \\ \vdots & & & & & & \end{pmatrix}.$$

- 2 → 2 particle interaction terms fill out the rest of the Hamiltonian matrix.

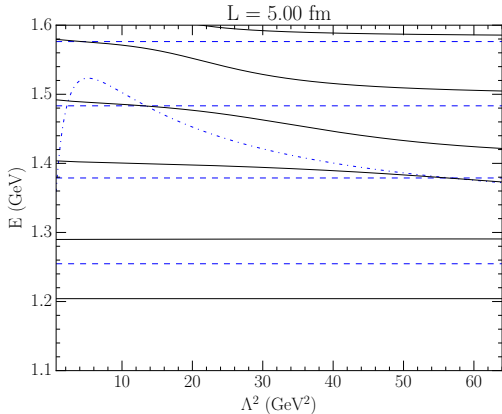
Finite Volume Eigenmode Solution

- Standard Lapack routines provide eigenmode solutions of

$$\langle i | H | j \rangle \langle j | E_\alpha \rangle = E_\alpha \langle i | E_\alpha \rangle,$$

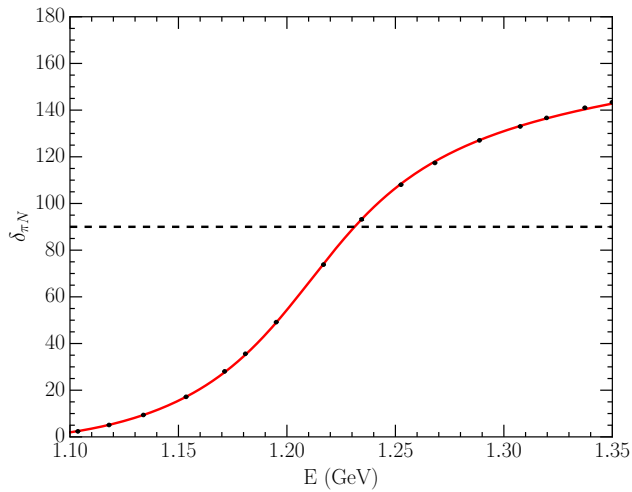
- where $|i\rangle$ and $|j\rangle$ are the non-interacting basis states,
- E_α is the energy eigenvalue, and
- $\langle i | E_\alpha \rangle$ is the eigenvector of the Hamiltonian matrix $\langle i | H | j \rangle$.

Energy eigenstates on an $L = 5$ fm lattice for different regulators

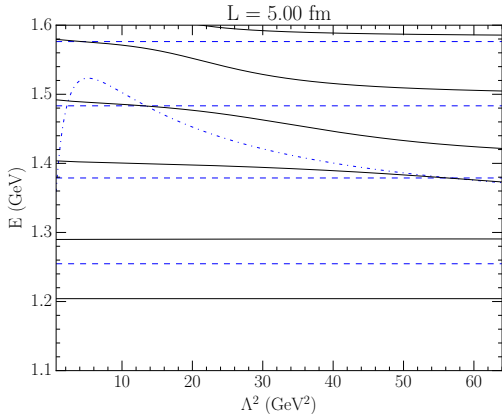


- Incorporation of the Lüscher formalism ensures energy eigenstates below 1.35 GeV are model independent.

P-wave πN phase shifts in the Δ channel - 1 πN channel

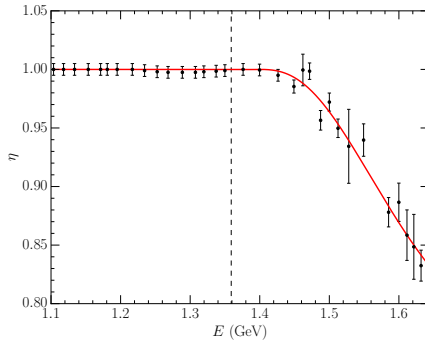
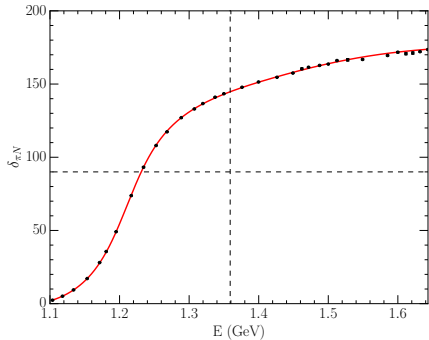


Energy eigenstates on an $L = 5$ fm lattice for different regulators

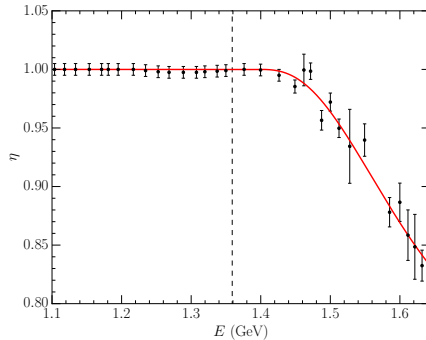
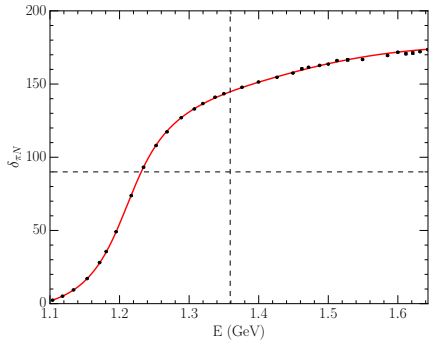


- Incorporation of the Lüscher formalism ensures energy eigenstates below 1.35 GeV are model independent.

P -wave πN scattering in the Δ channel - 2 channel πN and $\pi\Delta$

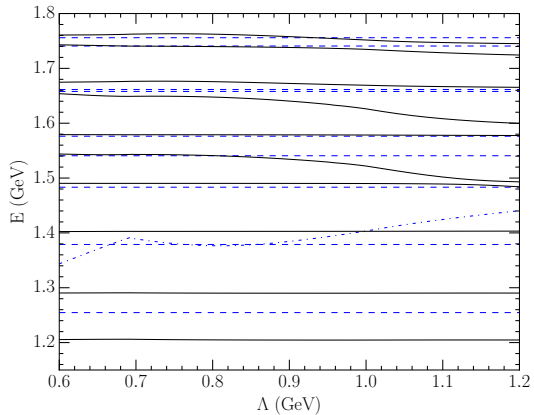


P -wave πN scattering in the Δ channel - 2 channel πN and $\pi\Delta$

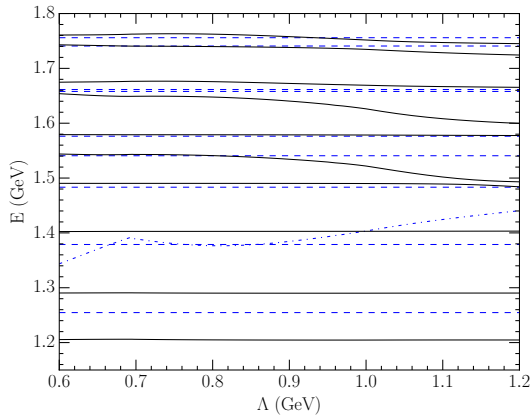


- Anticipate regulator independence to 1.7 GeV.

Energy eigenstates on an $L = 5$ fm lattice for different regulators

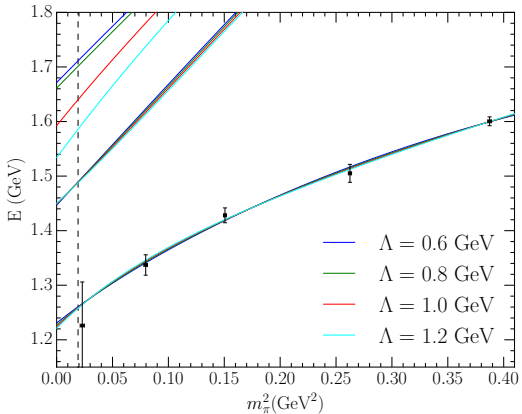


Energy eigenstates on an $L = 5$ fm lattice for different regulators



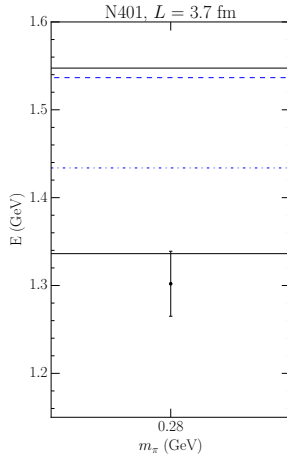
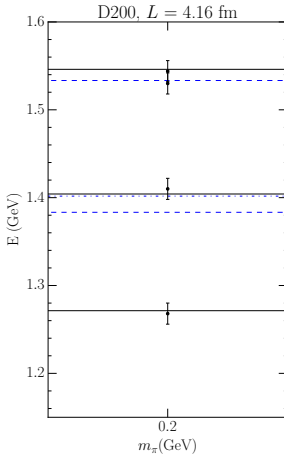
- πN scattering data alone is insufficient to uniquely constrain the Hamiltonian.

Mass dependence of energy eigenstates - Fit to PACS-CS Δ masses



- Lattice QCD results can constrain the Hamiltonian description of experimental data.

CLS Consortium finite-volume lattice energies of Δ -channel excitations

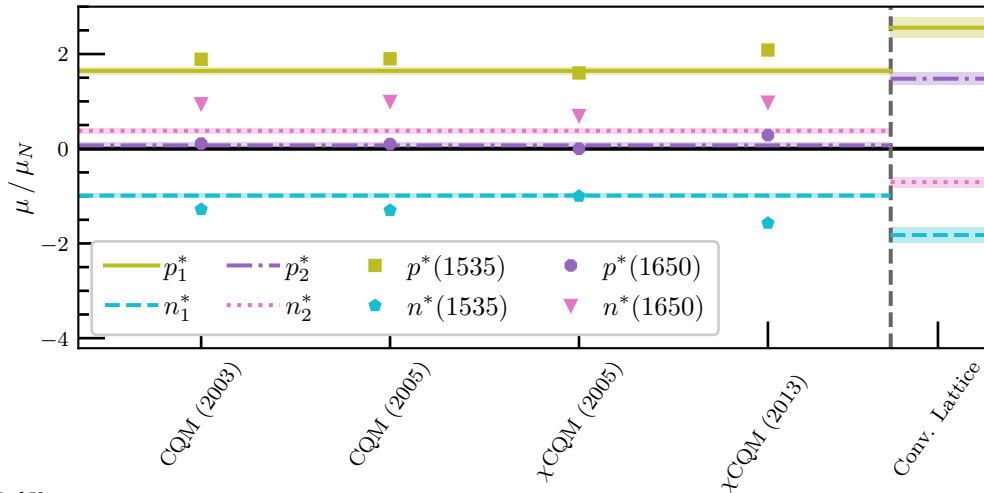


- C. Morningstar, et al. PoS **LATTICE2021** (2022), 170 [[arXiv:2111.07755 \[hep-lat\]](https://arxiv.org/abs/2111.07755)].
- C. W. Andersen, J. Bulava, B. Hörz and C. Morningstar, Phys. Rev. D **97** (2018) no.1, 014506 [[arXiv:1710.01557 \[hep-lat\]](https://arxiv.org/abs/1710.01557)].

Examination of low-lying odd-parity nucleon resonances

- Motivated by lattice QCD calculations of the electromagnetic form factors of the two low-lying odd-parity states.
- Parity-expanded variational analysis (PEVA) removes opposite-parity contaminants.
- Confirms quark model predictions for N^* magnetic moments.
- F. M. Stokes, W. Kamleh and D. B. L., Phys. Rev. D **102** (2020) 014507
[arXiv:1907.00177 [hep-lat]].

N^* Magnetic Moments and the constituent quark model



Model Calculation References

- CQM (2003)

W.-T. Chiang, S. N. Yang, M. Vanderhaeghen, and D. Drechsel, Magnetic dipole moment of the S 11 (1535) from the $\gamma p \rightarrow \gamma \eta p$ reaction, Nucl. Phys. **A723**, 205 (2003), nucl-th/0211061

- χ CQM (2005)

J. Liu, J. He, and Y. Dong, Magnetic moments of negative-parity low-lying nucleon resonances in quark models, Phys. Rev. **D71**, 094004 (2005).

- χ CQM (2013)

N. Sharma, A. Martinez Torres, K. Khemchandani, and H. Dahiya, Magnetic moments of the low-lying $1/2^-$ octet baryon resonances, Eur. Phys. J. **A49**, 11 (2013), arXiv:1207.3311

Examination of low-lying odd-parity nucleon resonances

- Motivated by lattice QCD calculations of the electromagnetic form factors of the two low-lying odd-parity states
 - Parity-expanded variational analysis (PEVA) removes opposite-parity contaminants.
 - Confirms quark model predictions for N^* magnetic moments.
 - F. M. Stokes, W. Kamleh and D. B. L., Phys. Rev. D **102** (2020) 014507 [arXiv:1907.00177 [hep-lat]].

Examination of low-lying odd-parity nucleon resonances

- Motivated by lattice QCD calculations of the electromagnetic form factors of the two low-lying odd-parity states
 - Parity-expanded variational analysis (PEVA) removes opposite-parity contaminants.
 - Confirms quark model predictions for N^* magnetic moments.
 - F. M. Stokes, W. Kamleh and D. B. L., Phys. Rev. D **102** (2020) 014507 [arXiv:1907.00177 [hep-lat]].
- Perform the first HEFT analysis with two bare basis states
 - One associated with the $N^*(1535)$ and the other with the $N^*(1650)$.

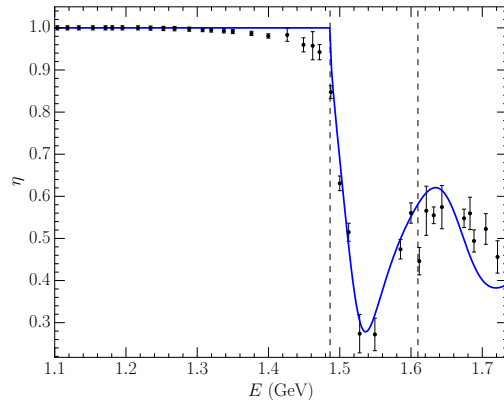
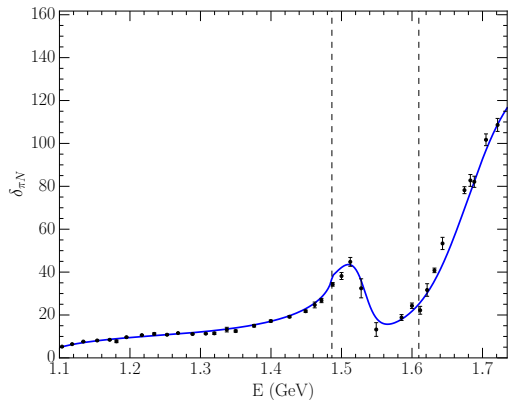
Examination of low-lying odd-parity nucleon resonances

- Motivated by lattice QCD calculations of the electromagnetic form factors of the two low-lying odd-parity states
 - Parity-expanded variational analysis (PEVA) removes opposite-parity contaminants.
 - Confirms quark model predictions for N^* magnetic moments.
 - F. M. Stokes, W. Kamleh and D. B. L., Phys. Rev. D **102** (2020) 014507 [arXiv:1907.00177 [hep-lat]].
- Perform the first HEFT analysis with two bare basis states
 - One associated with the $N^*(1535)$ and the other with the $N^*(1650)$.
- Includes three meson-baryon scattering channels, πN , ηN , and $K\Lambda$.

Examination of low-lying odd-parity nucleon resonances

- Motivated by lattice QCD calculations of the electromagnetic form factors of the two low-lying odd-parity states
 - Parity-expanded variational analysis (PEVA) removes opposite-parity contaminants.
 - Confirms quark model predictions for N^* magnetic moments.
 - F. M. Stokes, W. Kamleh and D. B. L., Phys. Rev. D **102** (2020) 014507 [arXiv:1907.00177 [hep-lat]].
- Perform the first HEFT analysis with two bare basis states
 - One associated with the $N^*(1535)$ and the other with the $N^*(1650)$.
- Includes three meson-baryon scattering channels, πN , ηN , and $K\Lambda$.
- 21 parameter fit provides an excellent characterisation of the data.
 - Pole positions agree with PDG.

Phase shift and inelasticity for the low-lying odd-parity spin-1/2 nucleon resonances



- WI08 single-energy data from SAID.
- Vertical lines indicate the opening of the ηN and $K\Lambda$ thresholds.

Finite Volume Eigenmode Solution

- Standard Lapack routines provide eigenmode solutions of

$$\langle i | H | j \rangle \langle j | E_\alpha \rangle = E_\alpha \langle i | E_\alpha \rangle.$$

- Eigenvector $\langle i | E_\alpha \rangle$ describes the composition of the eigenstate $|E_\alpha\rangle$ in terms of the basis states $|i\rangle$ with

$$|i\rangle = |B_0\rangle, \quad |\pi N, k_0\rangle, \quad |\pi N, k_1\rangle, \quad \dots | \eta N, k_0\rangle, \quad |\eta N, k_1\rangle, \quad \dots .$$

Finite Volume Eigenmode Solution

- Standard Lapack routines provide eigenmode solutions of

$$\langle i | H | j \rangle \langle j | E_\alpha \rangle = E_\alpha \langle i | E_\alpha \rangle.$$

- Eigenvector $\langle i | E_\alpha \rangle$ describes the composition of the eigenstate $| E_\alpha \rangle$ in terms of the basis states $| i \rangle$ with

$$| i \rangle = | B_0 \rangle, \quad | \pi N, k_0 \rangle, \quad | \pi N, k_1 \rangle, \quad \dots | \eta N, k_0 \rangle, \quad | \eta N, k_1 \rangle, \quad \dots .$$

- The overlap of the bare basis state $| B_0 \rangle$ with eigenstate $| E_\alpha \rangle$,

$$\langle B_0 | E_\alpha \rangle,$$

is of particular interest,

Finite Volume Eigenmode Solution

- In Hamiltonian EFT, the only localised basis state is the bare basis state.

Finite Volume Eigenmode Solution

- In Hamiltonian EFT, the only localised basis state is the bare basis state.
- Bär has highlighted how χ PT provides an estimate of the direct coupling of a smeared nucleon interpolating field to a non-interacting πN (basis) state.

$$\frac{3}{16} \frac{1}{(f_\pi L)^2 E_\pi L} \left(\frac{E_N - M_N}{E_N} \right) \sim 10^{-3},$$

relative to the ground state.

Finite Volume Eigenmode Solution

- In Hamiltonian EFT, the only localised basis state is the bare basis state.
- Bär has highlighted how χ PT provides an estimate of the direct coupling of a smeared nucleon interpolating field to a non-interacting πN (basis) state.

$$\frac{3}{16} \frac{1}{(f_\pi L)^2 E_\pi L} \left(\frac{E_N - M_N}{E_N} \right) \sim 10^{-3},$$

relative to the ground state.

- Conclude the smeared interpolating fields of lattice QCD are associated with the bare basis states of HEFT

$$\bar{\chi}(0) |\Omega\rangle \simeq |B_0\rangle ,$$

Finite Volume Eigenmode Solution

- In Hamiltonian EFT, the only localised basis state is the bare basis state.
- Bär has highlighted how χ PT provides an estimate of the direct coupling of a smeared nucleon interpolating field to a non-interacting πN (basis) state.

$$\frac{3}{16} \frac{1}{(f_\pi L)^2 E_\pi L} \left(\frac{E_N - M_N}{E_N} \right) \sim 10^{-3},$$

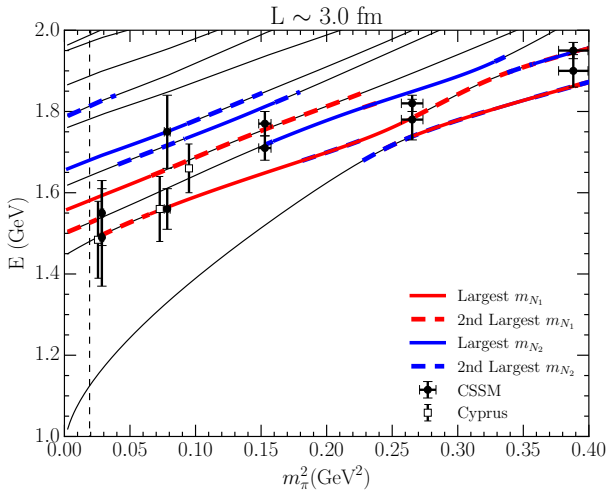
relative to the ground state.

- Conclude the smeared interpolating fields of lattice QCD are associated with the bare basis states of HEFT

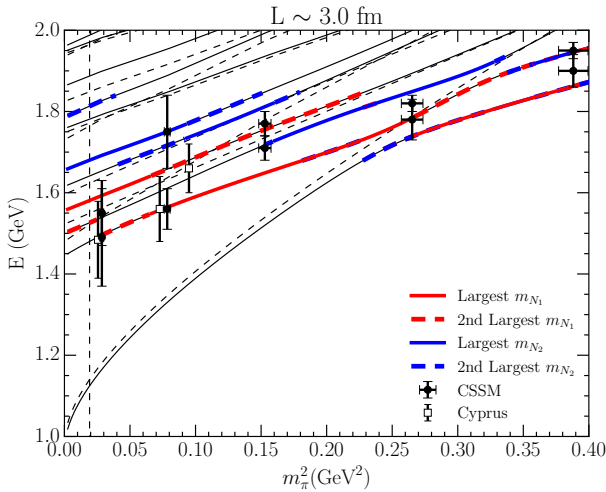
$$\bar{\chi}(0) |\Omega\rangle \simeq |B_0\rangle,$$

- Thus, element $\langle B_0 | E_\alpha \rangle$ of the eigenvector governs the likelihood of observing eigenstate $|E_\alpha\rangle$.

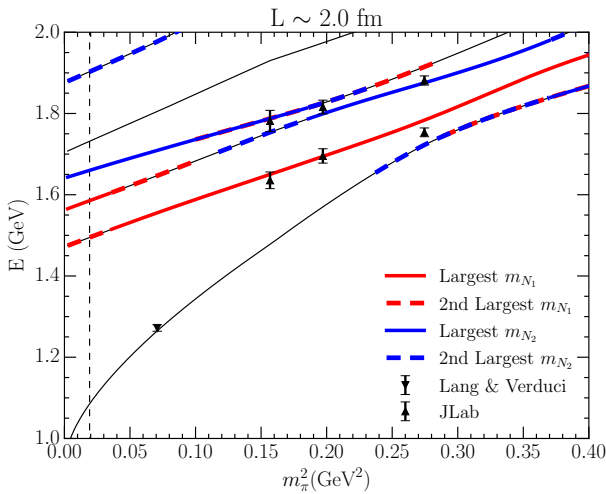
Finite-volume $L = 3$ fm energy levels for low-lying odd-parity spin-1/2 nucleons



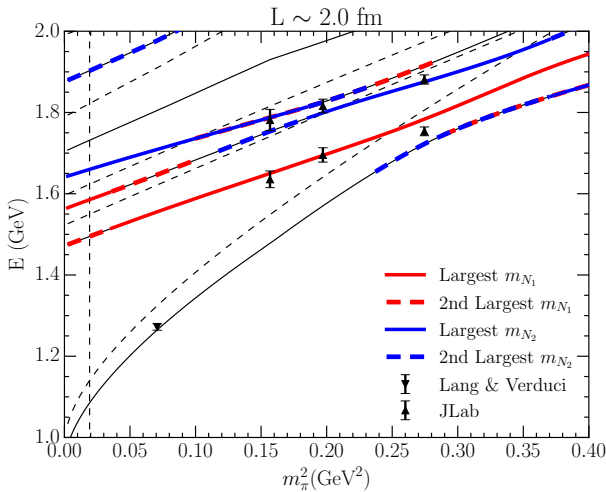
Finite-volume $L = 3$ fm energy levels for low-lying odd-parity spin-1/2 nucleons



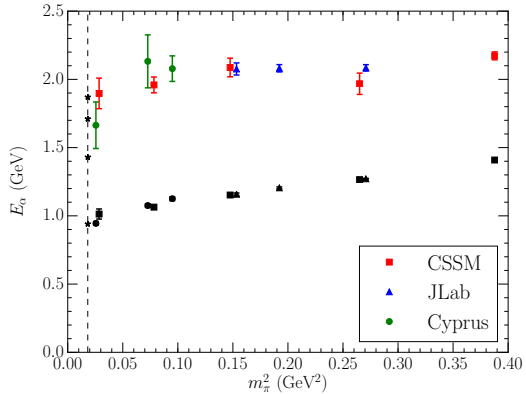
Finite-volume $L = 2$ fm energy levels for low-lying odd-parity spin-1/2 nucleons



Finite-volume $L = 2$ fm energy levels for low-lying odd-parity spin-1/2 nucleons



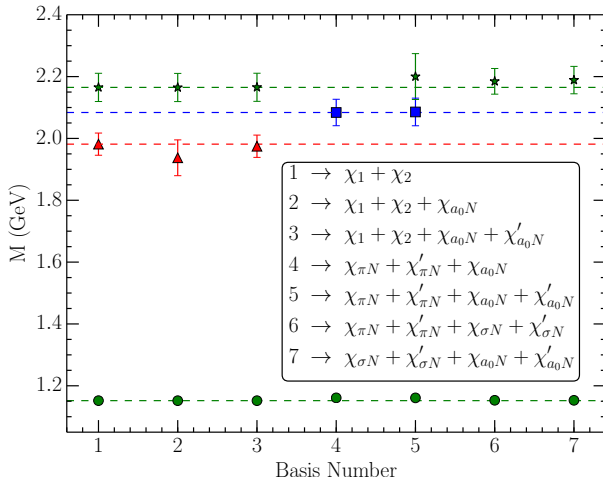
Where is the Roper resonance?



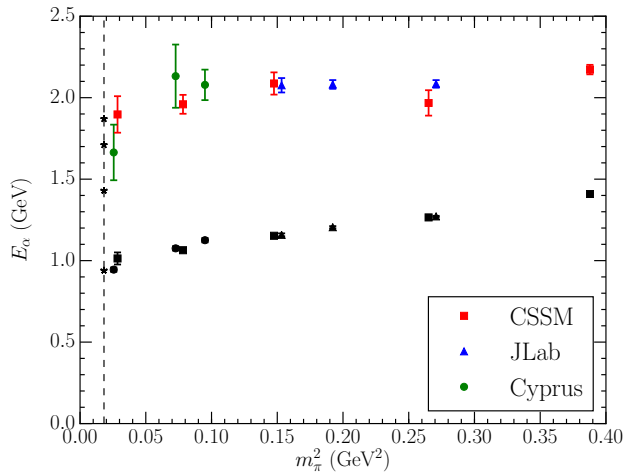
- CSSM: Z. W. Liu, *et al.* [CSSM], Phys. Rev. D **95**, 034034 (2017) arXiv:1607.04536 [nucl-th]
- Cyprus: C. Alexandrou, *et al.* (AMIAS), Phys. Rev. D **91**, 014506 (2015) arXiv:1411.6765 [hep-lat]
- JLab: R. G. Edwards, *et al.* [HSC] Phys. Rev. D **84**, 074508 (2011) [arXiv:1104.5152 [hep-ph]].

Search for low-lying lattice QCD eigenstates in the Roper regime

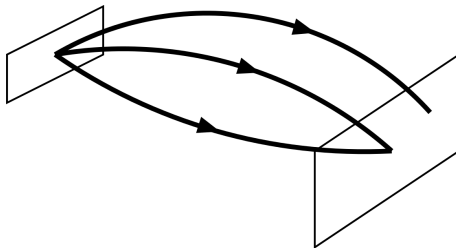
A. L. Kiratidis, et al., [CSSM] Phys. Rev. D 95, no. 7, 074507 (2017) [arXiv:1608.03051 [hep-lat]].



Have we seen the $2s$ excitation of the quark model?

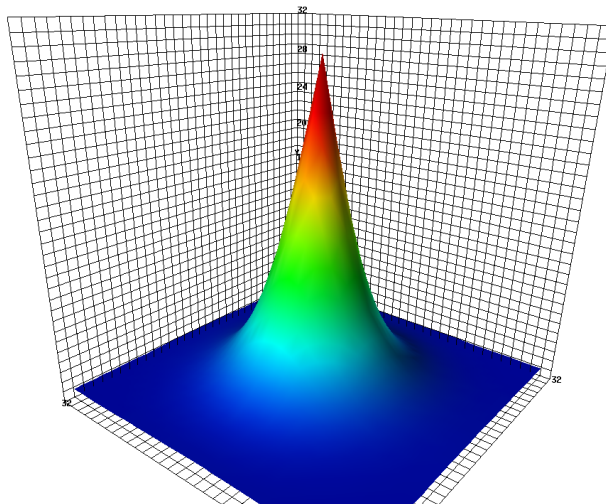


Landau-Gauge Wave functions from the Lattice

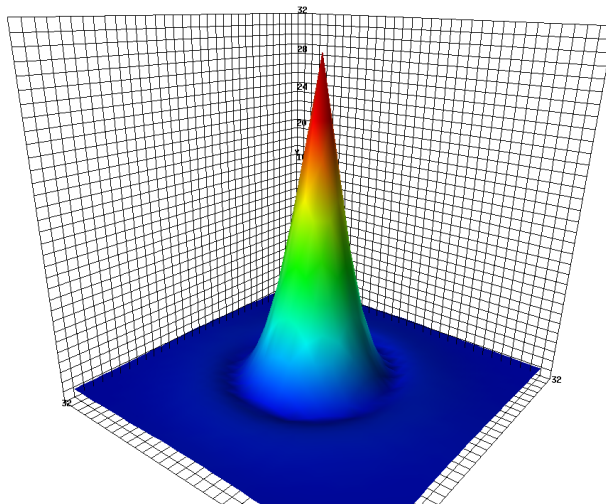


- Measure the *overlap* of the annihilation operator with the state as a function of the quark positions.

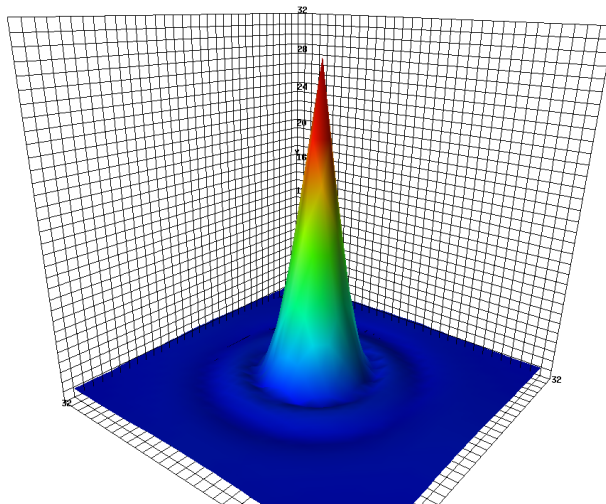
d-quark probability density in ground state proton [CSSM]



d-quark probability density in 1st excited state of proton [CSSM]

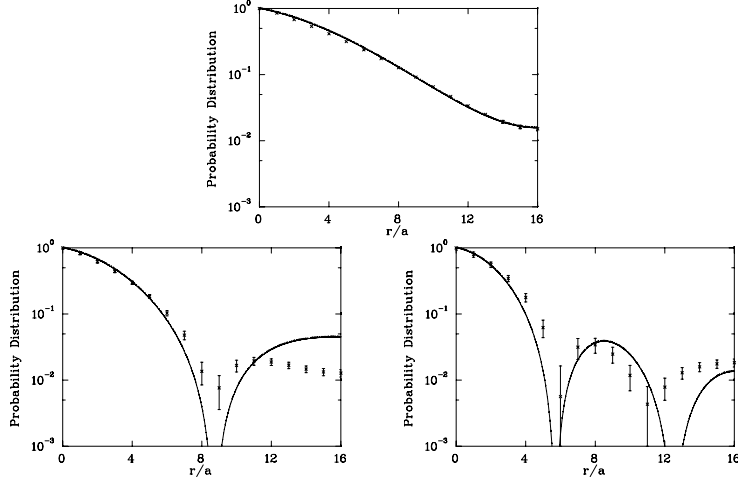


d -quark probability density in $N = 3$ excited state of proton [CSSM]

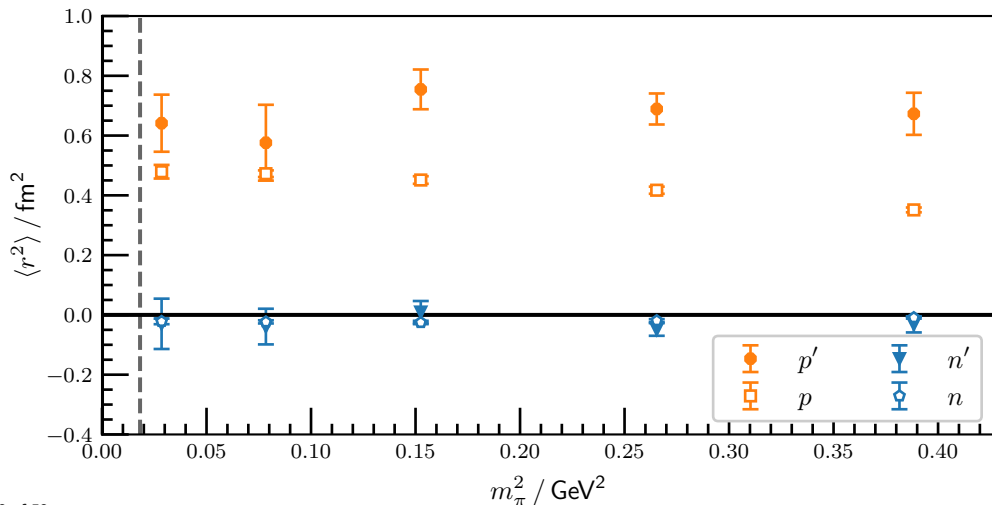


Comparison with the Simple Quark Model [CSSM]

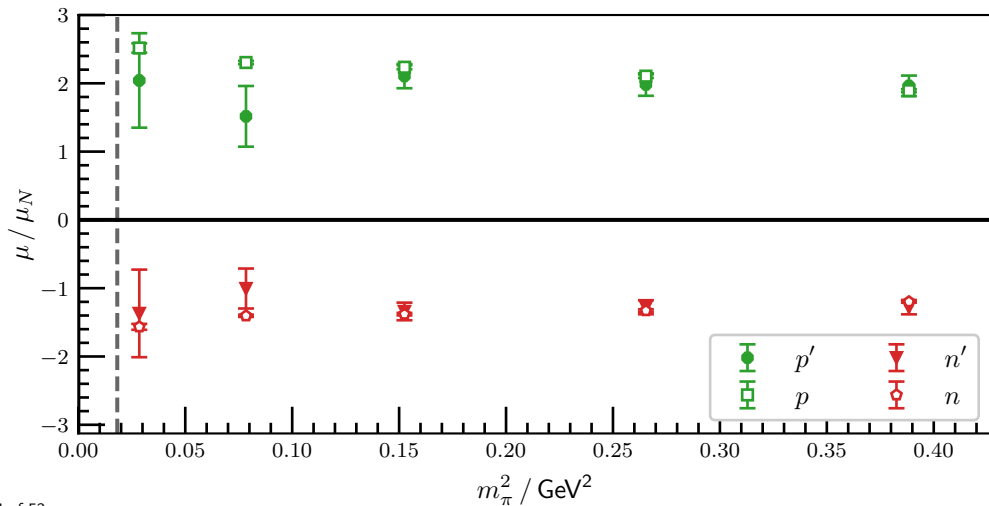
D. S. Roberts, W. Kamleh and D. B. Leinweber, Phys. Lett. B 725, 164 (2013) [arXiv:1304.0325 [hep-lat]].



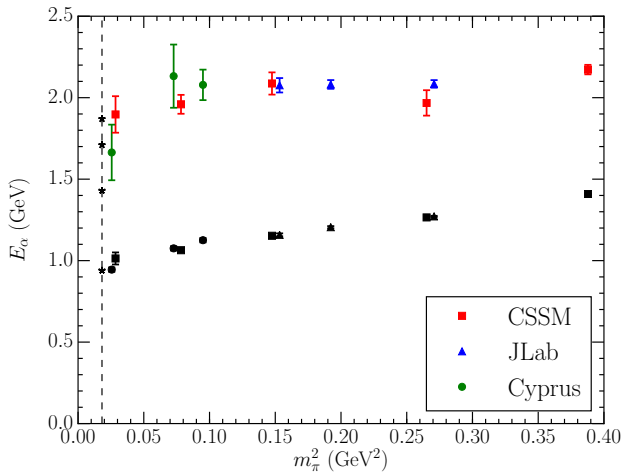
First positive-parity excitation: Charge Radii



First positive-parity excitation: Magnetic moments

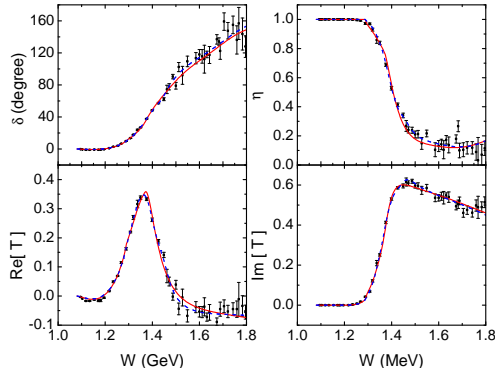


Are these lattice results consistent with the Roper Resonance?



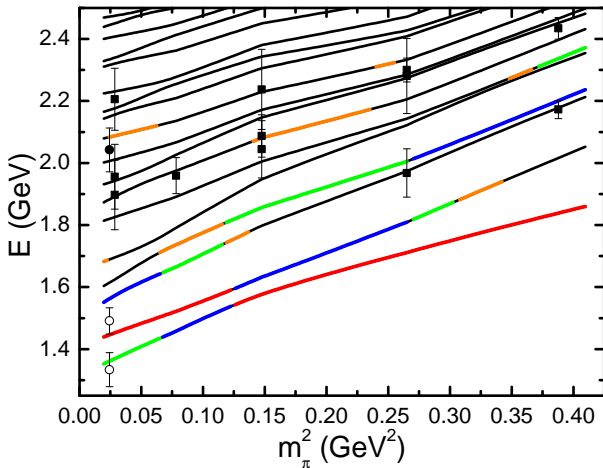
Positive-parity Nucleon Spectrum: Bare Roper Case with $m_0 = 1.7$ GeV

- Consider πN , $\pi\Delta$ and σN channels, dressing a bare state.
- Fit to phase shift and inelasticity. (dashed blue curve)



- Fit yields two poles in the region of the PDG estimate $1365 \pm 15 - i 95 \pm 15$ MeV.

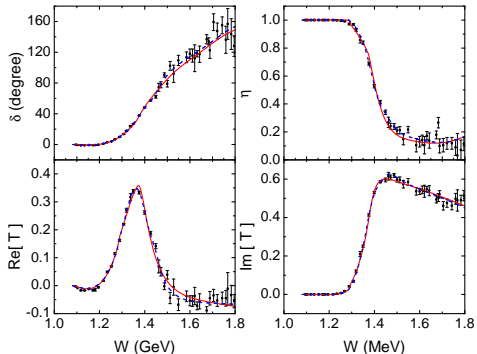
1.7 GeV Bare Roper: Hamiltonian Model N' Spectrum



Positive-parity Nucleon Spectrum: Bare Roper Case with $m_0 = 2.0$ GeV

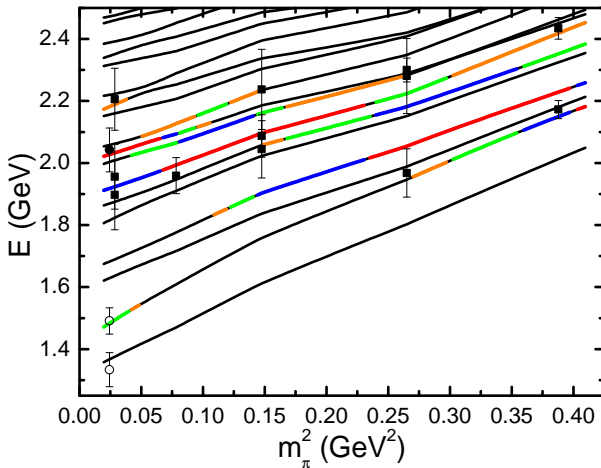
J. j. Wu, et al. [CSSM], arXiv:1703.10715 [nucl-th]

- Consider πN , $\pi\Delta$ and σN channels, dressing a bare state.
- Fit to phase shift and inelasticity. (red curve)

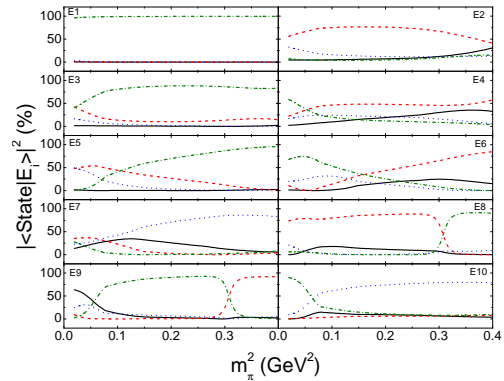
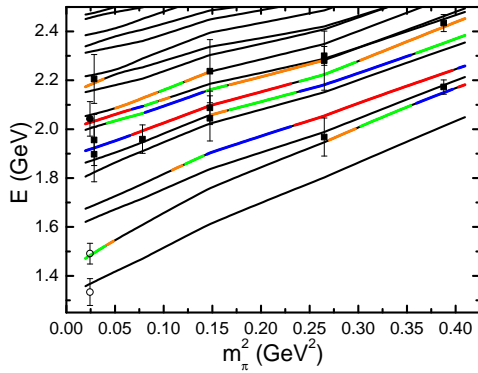


- Fit yields a pole at $1393 - i 167$ MeV \sim PDG estimate $1365 \pm 15 - i 95 \pm 15$ MeV.

2.0 GeV Bare Roper: Hamiltonian Model N' Spectrum



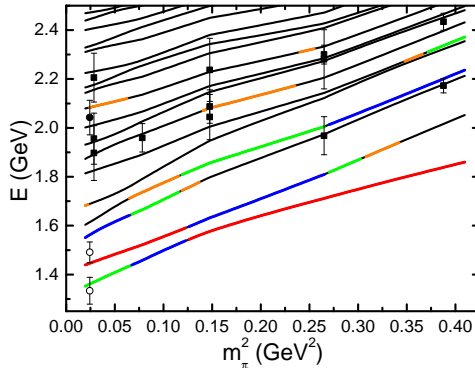
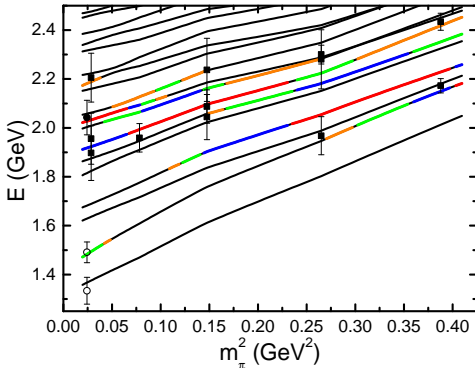
2.0 GeV Bare Roper: Hamiltonian Model N' Spectrum



πN , $\pi \Delta$ and σN channels, dressing a bare state.

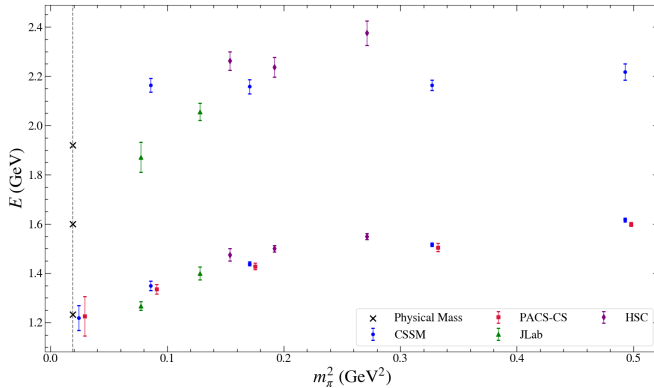
C. B. Lang, L. Leskovec, M. Padmanath and S. Prelovsek, Phys. Rev. D 95, no. 1, 014510 (2017) [arXiv:1610.01422 [hep-lat]].

Two different descriptions of the Roper resonance



(left) Resonance generated by strong rescattering in meson-baryon channels.
 (right) Meson dressings of a quark-model like core.

Δ -baryon spectrum from lattice QCD



HSC: J. Bulava, *et al.*, Phys. Rev. D **82** (2010) 014507 [arXiv:1004.5072 [hep-lat]].

JLab: T. Khan, D. Richards and F. Winter, Phys. Rev. D **104** (2021) 034503 [arXiv:2010.03052 [hep-lat]].

PACS-CS: S. Aoki *et al.* [PACS-CS], Phys. Rev. D **79** (2009) 034503 [arXiv:0807.1661 [hep-lat]].

Conclusions

- Hamiltonian Effective Field Theory (HEFT)
 - Nonperturbative extension of chiral effective field theory aimed at resonance physics.
 - Incorporates the Lüscher formalism.
 - Connects infinite-volume scattering observables to finite-volume Lattice QCD.

Conclusions

- Hamiltonian Effective Field Theory (HEFT)
 - Nonperturbative extension of chiral effective field theory aimed at resonance physics.
 - Incorporates the Lüscher formalism.
 - Connects infinite-volume scattering observables to finite-volume Lattice QCD.
 - Connects lattice results at different quark masses within a single formalism.

Conclusions

- Hamiltonian Effective Field Theory (HEFT)
 - Nonperturbative extension of chiral effective field theory aimed at resonance physics.
 - Incorporates the Lüscher formalism.
 - Connects infinite-volume scattering observables to finite-volume Lattice QCD.
 - Connects lattice results at different quark masses within a single formalism.
 - Provides insight into the composition of energy eigenstates.
 - Facilitates an understanding of lattice QCD results.

Conclusions

- Hamiltonian Effective Field Theory (HEFT)
 - Nonperturbative extension of chiral effective field theory aimed at resonance physics.
 - Incorporates the Lüscher formalism.
 - Connects infinite-volume scattering observables to finite-volume Lattice QCD.
 - Connects lattice results at different quark masses within a single formalism.
 - Provides insight into the composition of energy eigenstates.
 - Facilitates an understanding of lattice QCD results.
 - With lattice QCD constraints, HEFT provides deep insight into resonance structure.

Conclusions

- Hamiltonian Effective Field Theory (HEFT)
 - Nonperturbative extension of chiral effective field theory aimed at resonance physics.
 - Incorporates the Lüscher formalism.
 - Connects infinite-volume scattering observables to finite-volume Lattice QCD.
 - Connects lattice results at different quark masses within a single formalism.
 - Provides insight into the composition of energy eigenstates.
 - Facilitates an understanding of lattice QCD results.
 - With lattice QCD constraints, HEFT provides deep insight into resonance structure.
- Δ Resonance: illustrate Lüscher constraints and the role of lattice QCD constraints.

Conclusions

- Hamiltonian Effective Field Theory (HEFT)
 - Nonperturbative extension of chiral effective field theory aimed at resonance physics.
 - Incorporates the Lüscher formalism.
 - Connects infinite-volume scattering observables to finite-volume Lattice QCD.
 - Connects lattice results at different quark masses within a single formalism.
 - Provides insight into the composition of energy eigenstates.
 - Facilitates an understanding of lattice QCD results.
 - With lattice QCD constraints, HEFT provides deep insight into resonance structure.
- Δ Resonance: illustrate Lüscher constraints and the role of lattice QCD constraints.
- Odd-parity $N^*(1535)$ and $N^*(1650)$ Resonances:
 - Knowledge of eigenstate composition can be used to understand the states observed.
 - Dominated by a quark-core bare state dressed by meson degrees of freedom.

Conclusions

- Hamiltonian Effective Field Theory (HEFT)
 - Nonperturbative extension of chiral effective field theory aimed at resonance physics.
 - Incorporates the Lüscher formalism.
 - Connects infinite-volume scattering observables to finite-volume Lattice QCD.
 - Connects lattice results at different quark masses within a single formalism.
 - Provides insight into the composition of energy eigenstates.
 - Facilitates an understanding of lattice QCD results.
 - With lattice QCD constraints, HEFT provides deep insight into resonance structure.
- Δ Resonance: illustrate Lüscher constraints and the role of lattice QCD constraints.
- Odd-parity $N^*(1535)$ and $N^*(1650)$ Resonances:
 - Knowledge of eigenstate composition can be used to understand the states observed.
 - Dominated by a quark-core bare state dressed by meson degrees of freedom.
- Roper $N(1440)$ Resonance: Arises from dynamical coupled-channel effects.
 - Lattice QCD results constrain the HEFT description of experimental data.
 - State composition matches when the $2s$ excitation of the quark model sits at ~ 2 GeV.